Lab 3 - Report 2

# Second Order Filters

Matteo Zortea, Elena Acinapura

October 2020

# Contents

# Introduction

In electronics, filters are circuits designed to select some ranges of frequency and reject others. Mainly, we can classify filters into four different categories depending on their behaviour over the whole frequency spectrum:

- Low-pass filters attenuate signals over a critical frequency
- High-pass filters attenuate signals under a critical frequency
- Band-pass filters attenuate signals below a first critical frequency and above a second critical frequency
- Band-stop filters (or notch filters) attenuate signal within two critical frequencies

In addition, all the above types of filters can be implemented by using passive components (passive filters) or by active components (active filters). We call *order* of the filter the order of the pole in the transfer function that determines the critical frequency of the circuit.
In this experience we analyzed and compared different implementations of a second-order low-pass filter using both passive and active components. We analyzed the transfer function of each configuration comparing measured data with a theoretical model and we analyzed the filters' stability by looking at their impulse response.

# 1 Experimental procedure and theoretical prediction

Let us briefly illustrate the experimental procedure that was adopted to test the behaviour of the following circuits, and explain how the theoretical models were calculated.
To begin with, we measured the frequency response of the circuits: we chose 8 frequencies in the range 10 Hz – 2 kHz, we stimulated the circuits with a sinusoidal wave of 4 V peak-to-peak and the we measured both the input and output waveforms. We measured their peak-to-peak amplitudes and the time delay between them in order to extract the phase shift. The theoretical transfer function in the frequency domain, $\widetilde{G}(s)$, was calculated using Laplace impedances and by simply writing loop equations fro the circuits. some approximations have been necessary when the circuits included some op-amp, and those will be discussed in each section. $\widetilde{G}$ will be represented graphically together with the experimental data as a function of the frequency, by substituting $s = -i\omega = -i2\pi f$.
In addition to that, we also measured the impulse response of the circuits, i.e. the output signal when the circuit is stimulated by a $\delta$ function[1] signal. To obtain that, we used as input a narrow square wave, with an amplitude of 5 V, low frequency (between 30 and 50 Hz) and a duty of 0.5%. When the system receives a $\delta$ as input, the output is predicted to be exactly the inverse Laplace transform of $\widetilde{G}(s)$, let us call it $G(t)$. However, since it is obvious that the input signal is neither infinitely high, nor infinitely narrow as a $\delta$ should be, the real output will rather be the *convolution* between $G(t)$ and the input square wave $V_{in}(t)$. So we first calculated the function $G(t)$, and then calculated the expected output signal as

$$V_{out}(t) = (G * V_{in})(t) = 5\text{V} \int_{t-t_0}^{t} G(t')\,\mathrm{d}t' \tag{1}$$

where it was assumed that $V_{in}$ has constant value of 5 Vbetween $t = 0$ and $t = t_0$; $t_0$ can be calculated by knowing the frequency of the square wave, $f$, and its duty $d$, as

$$t_0 = \frac{d}{f} \tag{2}$$

And that's all about the methods we used, let us move to the circuits.

[1] Or, rather, distribution :)

# 2 Second-order Low Pass Filter

## 2.1 Configuration A

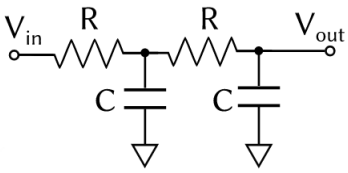


Figure 1: Configuration A

The first implementation of a second-order low pass filter, which is represented in figure 1, is just made of two RC cascade filters. For this and the following circuits, the values for $R$ and $C$ will be

$$R = 100\,\mathrm{k}\Omega \quad C = 10\,\mathrm{nF}$$

The **frequency response** of this circuit is simply calculated by writing the loop equations for the circuit without any approximation[2], thus obtaining

$$\widetilde{G}(s) = \frac{1}{\tau^2 s^2 + 3\tau s + 1} \tag{3}$$

where $\tau = RC$.

In the lab we measured the frequency response of the circuit; the experimental points were then compared with the theoretical model, which is represented by the curve obtained by substituting $s = -i\omega$ in eq.3. The comparison between data and model is represented in figure 2. As one can see, data and model agree to a good extent.
The points at the lower frequencies are slightly below the expected values, but this can be explained because the model doesn't take into account the presence of the oscilloscope. This would impact the circuit with ad additional capacitance of $C_{osc} \simeq 100\,\mathrm{pF}$ and a resistance of $R_{osc} \simeq 1\,\mathrm{M}\Omega$ in parallel between the output and the ground. The equivalent impedance of the oscilloscope and $C$ is

$$Z = \frac{R_{osc}}{1 + sR_{osc}C'} \tag{4}$$

where $C' = C + C_{osc}$.
Note that, because $C_{osc} \simeq 1\%C$, the presence of $C_{osc}$ is really negligible. On the opposite, the presence of $R_{osc}$ is not, and it lowers the gain of the circuit a low frequencies, where $Z \simeq R_{osc}$, hence producing the observed discrepancy.

We then calculated the **impulse response** of the circuit by finding the inverse Laplace transform of $\widetilde{G}$ of eq.3; this task can be accomplished without too much pain by factoring the denominator and then rewriting the whole fraction as the sum of two simple fractions:

$$\widetilde{G}(s) = \frac{1}{\tau^2(s_1 - s_2)}\left(\frac{1}{s - s_1} - \frac{1}{s - s_2}\right) \tag{5}$$

where $s_{1,2} = (-3 \pm \sqrt{5})/(2\tau)$ are the roots of the original denominator. Notice that they are both negative numbers, and we like that because it means that $\widetilde{G}$ has no pole in the RHP.
The inverse Laplace transform of the function 5 is then easily calculated by exploiting some properties of the Laplace transform, and one obtains

$$G(t) = \frac{1}{\tau^2(s_1 - s_2)}\left(e^{s_1 t} - e^{s_2 t}\right)\theta(t) \tag{6}$$

The measured output was compared with the convolution between the $G(t)$ of eq.6 and the square wave of the input, as was explained in section 1. The data and the model are represented in figure 3. One can see some discrepancy between them, not in the shape but rather in the height. Again, we were attributed this discrepancy to the effect of the oscilloscope, which was not taken into account. As we will see, in the

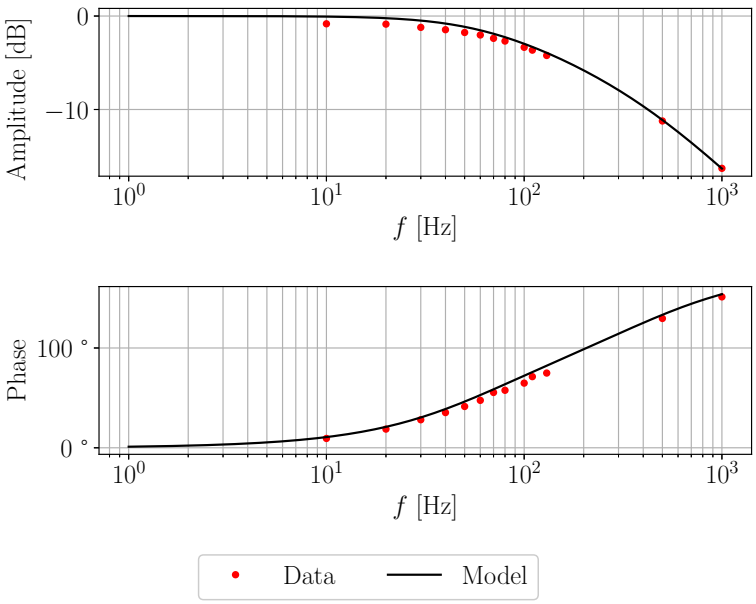


Figure 2: Frequency response of circuit 4

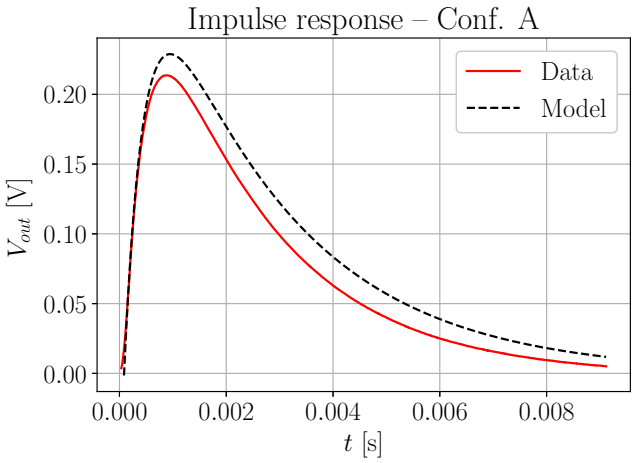


Figure 3: Experimental values and theoretical model of the output $V_{out}$ as a function of time, in response to a narrow square function.

next configurations, where the oscilloscope has smaller or no impact, the model will agree to the data much more, making us confident with our conjecture.

We calculated the output impedance of the circuit by "looking into the circuit from the output", obtaining

$$Z_{out} = \frac{R(2+\tau s)}{\tau^2 s^2 + 3\tau s + 1} \tag{7}$$

where we have ignored the oscilloscope to facilitate the calculations an because it doesn't affect much the result, since the overall impedance is dominated by the components of the circuit.

## 2.2 Configuration B

An improvement of the preceding configuration can be made by adding a buffer (or voltage follower) between the two filters stages, as showed in figure 4. In first approximation, by considering the operational amplifier as an ideal component with infinite input impedance and zero output impedance, we can neglect the current passing trough the amplifier so that the two filters work as two separated circuits, each one unaffected by the other. This results in a lower overall output impedance (the first stage is "hidden" by

[2] apart from neglecting the presence of a load, as is discussed later

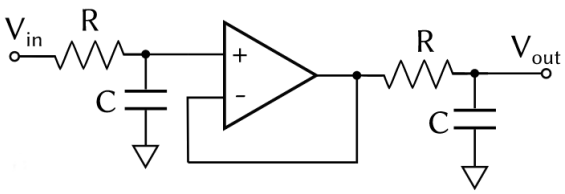


Figure 4: **Configuration B**

the buffer) and in a higher gain in the useful band.
The **transfer function** in the frequency domain is thus just the product of two equal low pass filters:

$$\widetilde{G}(s) = \left(\frac{1}{1+\tau s}\right)^2 \tag{8}$$

where, again, $\tau = RC$.

The comparison between measured data and theoretical model is presented graphically in figure 5.
The **impulse response** of the filter, i.e. the inverse transform of function 11 is easily calculated thanks

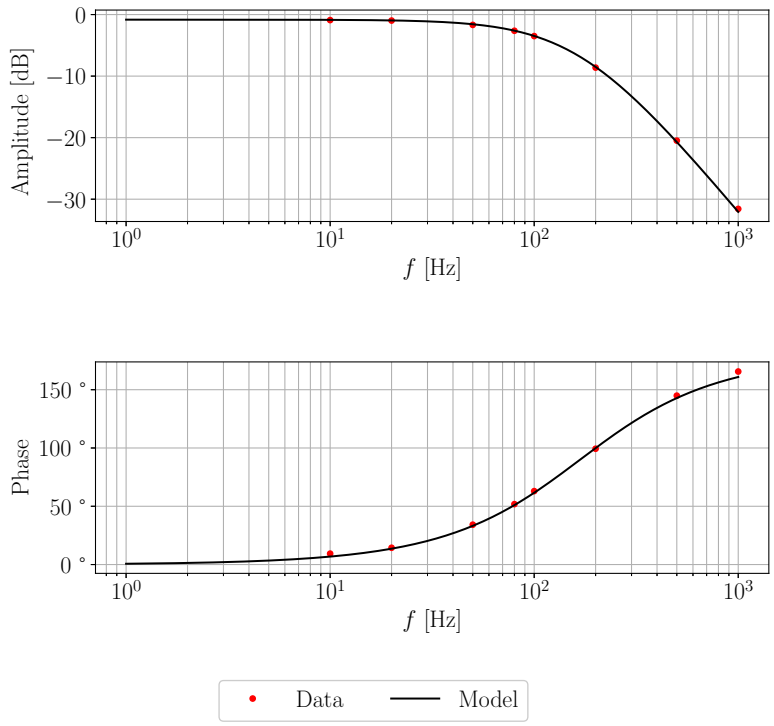


Figure 5: Frequency response of circuit 4

to some useful properties of the Laplace transform:

$$G(t) = \frac{t}{\tau^2} e^{-t/\tau}\theta(t) \tag{9}$$

Again, to verify the goodness of this model the circuit was stimulated with an impulse (i.e. a square wave), and the output was compared with the convolution of $G(t)$ and the input wave. This comparison is represented in figure 6, where one can see that now the model agrees much more with the data than it did in circuit A. This can be attributed to the op-amp that "separates" the two stages of the circuit, and thus makes the load (the oscilloscope) affect the gain only of the second low-pass filter. In this case the **output impedance** of the whole filter is completely determined by the parallel of the second stage capacitor and resistor's impedances since the operational amplifier is here considered as an infinite admittance component.[3] Thus it is

$$Z_{out} = \frac{R}{1+\tau s} \tag{10}$$

[3] Again, neglecting the oscilloscope's impedance.

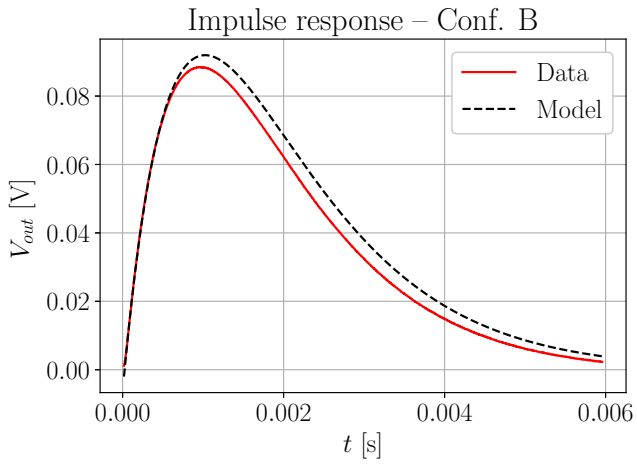


Figure 6: Experimental values and theoretical model of the output $V_{out}$ as a function of time, in response to a narrow square function.

## 2.3 Configuration C

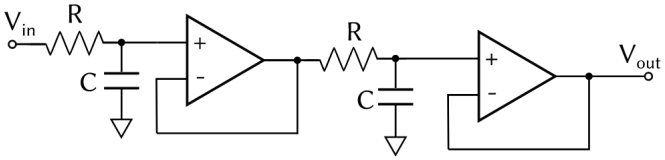


Figure 7: Configuration C

A further improvement of the filter design can be obtained by adding one more voltage follower at the output of the second filter stage as in figure 7. This leads to a reduction in the output impedance of the filter, hence "isolating" it from a hypothetical load (the oscilloscope and the coaxial cable in this case). The transfer function of the circuit remains the same as in the preceding section

$$\widetilde{G}(s) = \left(\frac{1}{1+\tau s}\right)^2 \tag{11}$$

where, again, $\tau = RC$.

Measurements are reported in figure 8 together with the theoretical model. Comparing it to the previous configurations we notice that the low-frequency gain has increased.

As for the frequency transfer function, also the **impulse response** of configuration C is the same of that of configuration B. Again, the convolution of function 9 with the input square wave has been calculated and then compared graphically with the output of the circuit. The result is represented in figure 9. As one can notice, the correspondence between experimental data and model is improved a lot, thanks to the effect of the second op-amp that isolates the circuit from the load.

We then tried to analyse the **asymptotic behaviour** of the filter by extracting the slope of the asymptotic line of the amplitude diagram in figure 8 and comparing it to the one expected for a second order filter, i.e. $-40$dB/decade. We can see that this fact is predicted by our model too, in the limit of large $\omega$ ($\omega \gg \omega_{crit}$):

$$|\widetilde{G}(s)|_{dB} = 20\log\left|\frac{1}{1+\tau s}\right|^2 = C_0 - 40\log\left|\frac{1}{\tau}+s\right| \approx C_0 - 40\log|s| \tag{12}$$

and by defining $x \equiv \log|s|$

$$|\tilde{G}(s)|_{\mathrm{dB}} = C_0 - 40x \tag{13}$$

The meaning of this relation is that a decrease of $40dB$ in the gain of the filter is expected for each decade of frequency, which is a unitary increment in the logarithmic scale.
The experimental slope we found by regression is

$$39 \pm 1\,\mathrm{dB/decade} \tag{14}$$

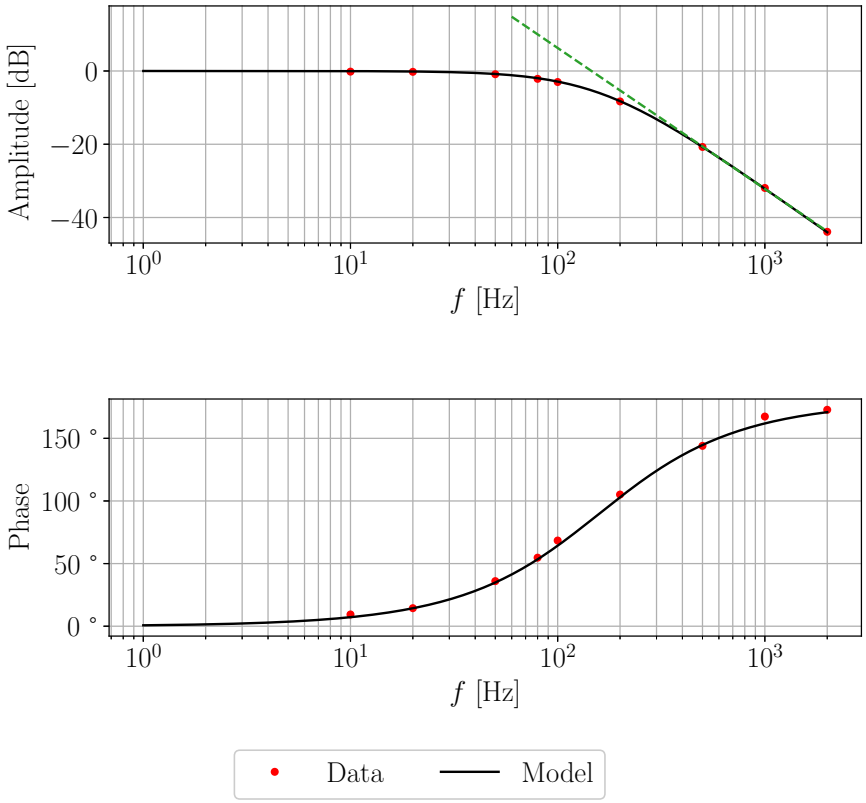


Figure 8: Frequency response of circuit C. The reason for the presence of the green line is explained at the of the section.

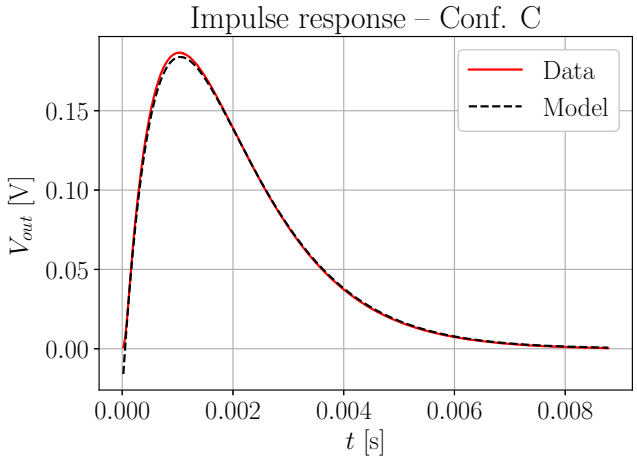


Figure 9: Experimental values and theoretical model of the output $V_{out}$ as a function of time, in response to a narrow square function.

and its related line is represented in figure 8. Even though we used only 3 points from the plot for the estimation, we obtained the expected result.
The steeper slope compared to the first-order filter's, indicates that the second-order filter cuts off "faster" after the critical point, resulting in a more accurate selection of the desired frequencies. Higher order filters can be obtained by adding more subsequent stages resulting in an even steeper asymptotic slope. Of course this implies also a higher energy demand.

Lastly, we thought that an overall comparison between the three circuits would be useful and would show the subsequent improvements. In table 2 we report a comparison of the gains at low frequencies; in

table **??** we list the output impedances; in figure 10 we compare graphically the three transfer functions and see how the useful frequency bandwidth is increased with the last two configurations.

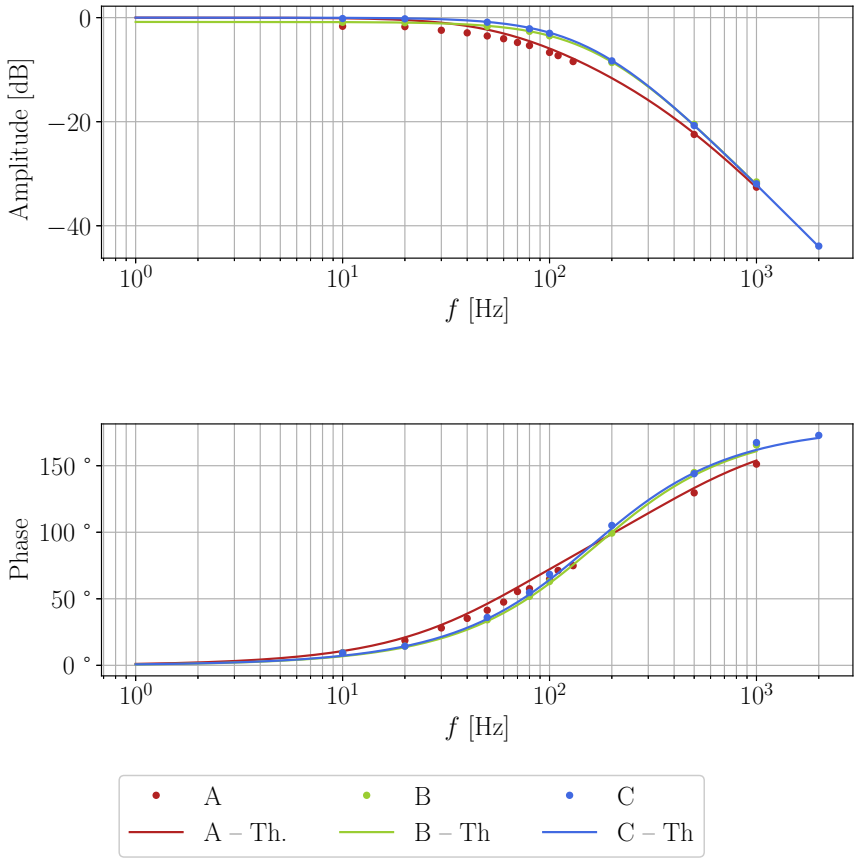


Figure 10: Comparison of the three transfer functions (data and theoretical model). The critical frequency increased with the use of the op-amps.

| Circuit | $\lvert\widetilde{G}\rvert$ (10 Hz) | $\lvert\widetilde{G}\rvert$ (20 Hz) | $\lvert\widetilde{G}\rvert$ (50 Hz) | $Z_{out}$ |
|---|---|---|---|---|
| **A** | −1.66 dB | −1.74 dB | −3.52 dB | $\frac{R(2+\tau s)}{\tau^2 s^2 + 3\tau s + 1}$ |
| **B** | −0.90 dB | −0.97 dB | −0.97 dB | $\frac{R}{1+\tau s}$ |
| **C** | −0.17 dB | −0.23 dB | −0.88 dB | $\approx 0$ |

Table 1: Low frequency gain and output impedance improvement.

# 3 Sallen-Key Filter

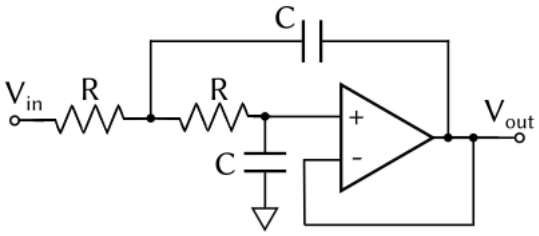


Figure 11: Sallen-Key circuit diagram.

In this section we present the analysis the circuit represented in figure 11, which is called *Sallen-Key* circuit and is too a second-order low-pass filter.

We calculated its **transfer function** in the frequency domain in the following way: firstly, we recognize that the op-amp is in the follower configuration, so that $V_{out} = V_+$; secondly, because the op-amp has a great input impedance, we neglect the current that flows into the op-amp; having in mind these two assumptions, we apply the Millman theorem to the potential between the two resistors. By expressing $V_{out}$ in terms of $V_{in}$ we obtain

$$\widetilde{G}(s) = \frac{1}{(1+\tau s)^2} \tag{15}$$

So the same transfer function of circuits B and C![4]. The theoretical transfer function is compared with the experimental points in figure 12.

The **impulse response** of the circuit is, as calculated before,

$$G(t) = \frac{t}{\tau^2} e^{-t/\tau}\theta(t) \tag{16}$$

and the convolution with the input square wave is compared with the experimental data in figure 13, where one can see that they are in good agreement.
The **output impedance** remains the same as the configuration C in the previous section, in first approximation determined by the operational-amplifier only, here considered an ideal component ($Z_{out} \approx 0\,\Omega$).

One may wonder which differences occur between filter C and the Sallen-Key filter. One advantage of the Sallen-Key filter is that its amplitude gain at low frequencies is higher than that of filter C, which was already higher than in circuits A and B. In table 2 their gains are compared to show that the difference becomes significant, especially at 10 Hz. Another great advantage of this configuration is that only one op-amp is needed, hence reducing power consumption.

| Circuit | $\lvert\widetilde{G}(s)\rvert$ (10 Hz) | $\lvert\widetilde{G}(s)\rvert$ (20 Hz) | $\lvert\widetilde{G}(s)\rvert$ (50 Hz) |
|---|---|---|---|
| **C** | −0.17 dB | −0.23 dB | −0.88 dB |
| **Sallen-Key** | −0.06 dB | −0.16 dB | −0.96 dB |

Table 2: **Low frequency gain improvement**. Here's a comparison between low-frequency gains of circuit C and the Sallen-Key.

[4] Amazing

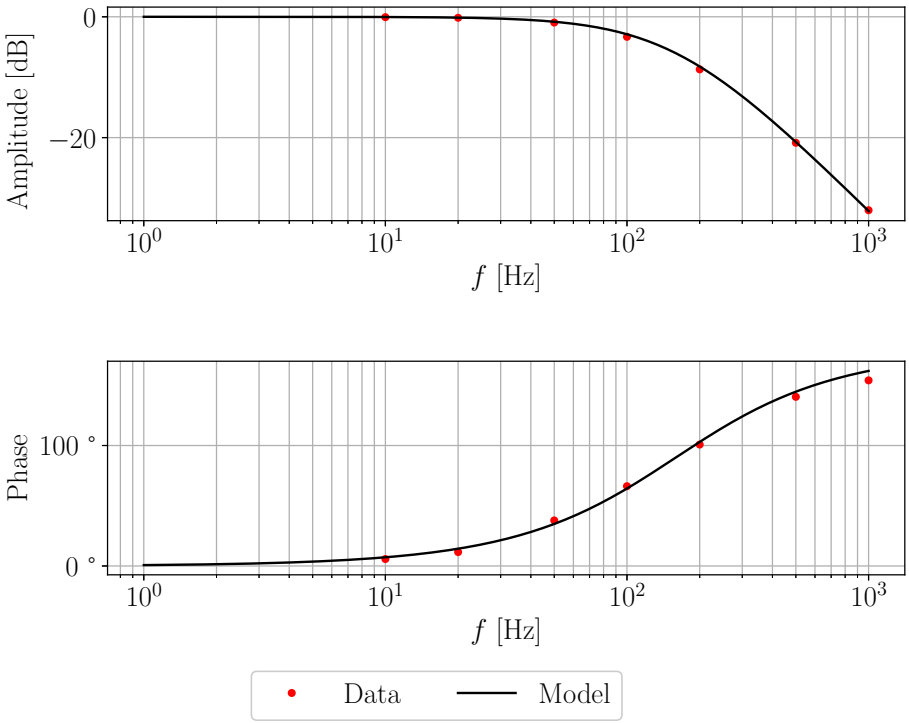


Figure 12: Frequency response of the Sallen-Key circuit.

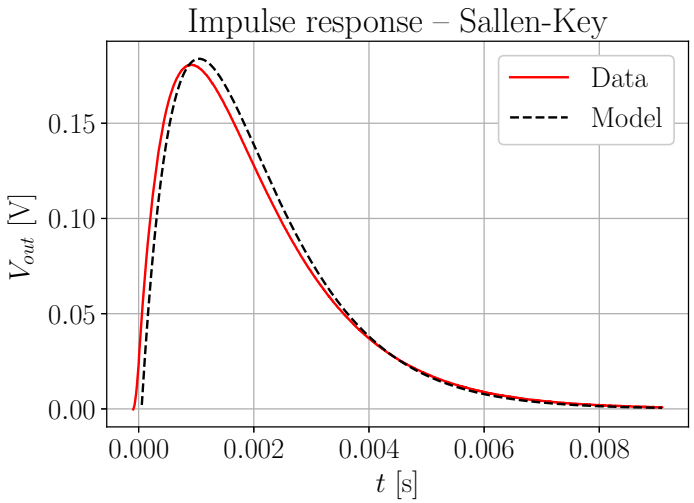


Figure 13: Impulse response of the Sallen-Key filter.

## Conclusion

In this experience we analyzed and compared different implementations of a second order low-pass filter. Starting from a simple circuit of two subsequent passive filters made with a capacitor and a resistance, we added appropriate buffers improving the circuit behaviour at low frequency and reducing the output impedance making the filter more suitable for further applications. After that we implemented a Sallen-Key filter, that is a circuit with only one op-amp and an even better behaviour in the desired band.
Stability of each circuit was tested by studying the impulse response, and all the implemented circuits resulted to be stable.